

Weyl nodal surfaces

Oğuz Türker and Sergej Moroz

Department of Physics, Technical University of Munich, 85748 Garching, Germany

We consider three-dimensional fermionic band theories that exhibit Weyl nodal surfaces defined as two-band degeneracies that form closed surfaces in the Brillouin zone. We demonstrate that topology ensures robustness of these objects under small perturbations of a Hamiltonian. This topological robustness is illustrated in several four-band models that exhibit nodal surfaces protected by unitary or anti-unitary symmetries. Surface states and Nielsen-Ninomiya doubling of nodal surfaces are also investigated.

I. INTRODUCTION

The advent of topological insulators in the last decade deepened our understanding of interplay of topology and symmetries in band insulators^{1,2}. This work culminated in the development of the ten-fold way classification of non-interacting gapped topological phases³ and the emergence of new symmetry protected topological phases of matter.

In last years the main interest in the field shifted towards systems with band degeneracies^{4–6}. In three dimensions the simplest and most well-studied are Weyl (semi)metals which are distinguished by isolated point-like two-band degeneracies in the Brillouin zone (BZ). Although in condensed matter physics Weyl points appeared first long time ago in the superfluid A phase of ³He^{7,8}, only recently Weyl semi(metals) were discovered experimentally^{9,10}. As long as inversion or time-reversal symmetry is broken, Weyl points appear generically. They are topological defects and cannot be gapped out individually but must be destroyed only via pairwise annihilation¹¹. Weyl (semi)metals exhibit robust phenomena such as chiral anomaly¹², anomalous Hall effect¹³ and zero-energy Fermi arc surface states¹⁴. More recently Weyl loop (semi)metals¹⁵, where two-band degeneracies take place on closed one-dimensional manifolds also attracted considerable attention. In contrast to Weyl points, nodal loops are not generic, but require some symmetry (such as chiral sub-lattice symmetry) to protect them. The defining feature of the Weyl loop is a nontrivial π Berry phase along any closed contour that links with it. In the semimetal regime, any boundary surface, where the loop projects non-trivially, supports zero-energy drumhead states^{15,16}.

One can make a step further and consider three-dimensional translation-invariant fermionic systems with Weyl nodal surfaces, where two bands touch each other on two-dimensional surfaces in the BZ. Recently nodal surfaces were predicted to appear in multi-band superconductors with broken time-reversal symmetry^{17,18} and also were found within the ten-fold way classification of gapless inversion-enriched systems¹⁹. Given a model with a nodal surface it is natural to ask if the nodal structure is robust under certain class of small perturbations of the Hamiltonian. Generically a perturbation can (i) open a gap everywhere and fully destroy the nodal object (ii)

gap it out partially leaving behind nodal loops and/or points²⁰, (iii) preserve the nodal surface and not open a gap anywhere on it. As we show in this paper the degree of robustness (i)-(iii) is determined by topology of the perturbed system. To see how it works, consider first a system which has only one nodal surface (tuned for convenience to the Fermi level), but no other gapless objects at the Fermi level such as additional Fermi surfaces, nodal loops or points. Now we enclose the nodal surface of the original model by a lower-dimensional ($d_m < 3$) manifold in the BZ (see Fig. 1). By construction, all

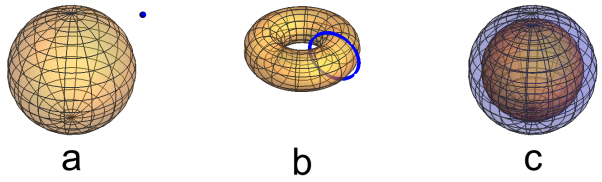


FIG. 1. Examples of (a) zero-, (b) one- and (c) two-dimensional enclosing manifolds (blue) around nodal surfaces (orange). Although technically a zero-dimensional manifold does not enclose the nodal surface with slight abuse of notation we still refer to it here as an enclosing manifold.

bands are gapped on the enclosing manifold. Imagine now that in the original model we can define a topological invariant (such as Chern number, winding number, \mathbb{Z}_2 invariant, etc) on this enclosing manifold. In this paper such invariant will be denoted as c_{d_m} , where the subscript specifies the dimension of the enclosing manifold. Importantly, the invariant does not change under a certain class of perturbation of the Hamiltonian and as we show now this has implications for the degree of robustness of the nodal surface under this class of perturbations. Previously, this set of ideas was introduced for determining the robustness of Weyl nodal loops^{21,22}.

First, we discuss topological invariants defined on a point ($d_m = 0$, Fig. 1 a) enclosing manifold. As long as such invariants are different for point manifolds placed inside and outside of the nodal surface in the BZ, the nodal surface cannot be gapped. The reason for that is the following: notice that on any imaginary one-dimensional trajectory in the BZ that connects the inner

and outer zero-dimensional manifolds there should be a point, where the energy gap closes allowing the topological invariant to change. In turn this ensures that no gap can open at any point of the nodal surface.

Second, consider nontrivial topological invariants defined on enclosing manifolds of dimension $d_m > 0$ (Fig. 1 b and c). These invariants do not fully protect the nodal surface, but guarantee that it cannot be fully gapped out by perturbations. Generically, a nodal line (nodal points) should survive in the perturbed system if $d_m = 1$ ($d_m = 2$). We can explain it by following similar arguments as before: in the unperturbed model compute the topological invariant on two enclosing manifolds, one being inside and another outside the nodal surface. Since the topological invariant on the interior manifold is necessarily trivial (the manifold can be shrunk to a point without encountering a band), a nontrivial invariant on the exterior manifold necessarily implies a nontrivial difference of the interior and exterior invariants which in turn guarantees a lower-dimensional nodal object in between the two enclosing manifolds in the perturbed system.

We emphasize that arguments presented above also imply robustness of general nodal surfaces, not necessarily tuned to the Fermi level. In the general case it is useful to formulate the above arguments in energy-momentum space, as detailed in Appendix A. Our analysis thus does not reduce to previous studies of robustness of Fermi surfaces^{8,23–25}.

To apply these ideas in practice, in this paper we investigate nodal surfaces protected by different mechanisms: (i) a nodal surface can be protected by a global internal symmetry. In this case any two bands that carry different quantum numbers with respect to the symmetry generically intersect on a two-dimensional surface in momentum space. Since in the presence of the symmetry the two bands cannot be hybridized, the nodal surface is protected against any small symmetry-preserving perturbations. (ii) in spirit of ten-fold way, Weyl nodal surfaces can be protected by anti-unitary symmetries. These nodal surfaces have already appeared in the literature^{17–19} and here we investigate their robustness. We analyze simple models that exhibit nodal surfaces protected by both mechanisms mentioned above, see Table I. The leitmotif of our construction is the following: we start from double-degenerate nodal points or nodal lines and split them in energy. The resulting continuum four-band models together with minimal lattice extensions thereof are used to analyze the physics of nodal surfaces and investigate their robustness. In particular, we identify symmetries that protect the nodal surface and construct appropriate topological invariants. In addition, we investigate Nielsen-Ninomiya doubling of nodal surfaces in the BZ and look for surface states and topological invariants that protect these states.

TABLE I. Spheric (S^2) and toric (T^2) nodal surfaces protected by unitary or anti-unitary symmetries. Nontrivial difference of topological invariants c_{d_m} defined on enclosing manifolds of dimension d_m ensures robustness of the nodal structure.

Sec.	Nodal object	Symmetry	Topological invariant c_{d_m}		
			$d_m = 0$	$d_m = 1$	$d_m = 2$
II A	S^2	$U(1)$	\mathbb{Z}	-	\mathbb{Z}
II B	T^2	$U(1)$	\mathbb{Z}	-	-
III A	S^2	PC	\mathbb{Z}_2	-	\mathbb{Z}
III B	T^2	$PC + PT$	\mathbb{Z}_2	\mathbb{Z}	-

II. NODAL SURFACES PROTECTED BY UNITARY $U(1)$ SYMMETRY

In this section we construct and investigate non-interacting fermionic four-band models that exhibit nodal surfaces protected by an internal unitary $U(1)$ symmetry.

A. Nodal sphere

Given the set of four-by-four Dirac matrices γ^μ that satisfy the Clifford algebra $\{\gamma^\mu, \gamma^\nu\} = 2\eta^{\mu\nu}$ with the Minkowski metric $\eta^{\mu\nu}$ and $\mu, \nu = 0, x, y, z$, we first define $\alpha^i = \gamma^0 \gamma^i$ and $\gamma^5 = i\gamma^0 \gamma^x \gamma^y \gamma^z$. Now consider the massless Dirac Hamiltonian perturbed by a γ^5 term

$$\mathcal{H}(\mathbf{k}) = k_i \alpha^i - \lambda \gamma^5, \quad (1)$$

where k_i is momentum and $\lambda \in \mathbb{R}$. Since $[\gamma^5, \mathcal{H}] = 0$, the model has an internal $U(1)$ symmetry²⁶ generated by the matrix γ^5 . In this paper we use the chiral representation of the Dirac matrices resulting in $\alpha^i = \sigma^z \otimes \tau^i$ and $\gamma^5 = -\sigma^z \otimes \tau^0$. The last term in Eq. (1) splits the Dirac point at $\mathbf{k} = 0$ into a pair of Weyl points of opposite chirality by separating them in energy by 2λ . This model appeared in the context of studies of the chiral magnetic effect²⁷. The energy spectrum

$$E(k) = \pm k \pm \lambda \quad (2)$$

exhibits a band degeneracy at the Fermi level $E = 0$ on a sphere defined by $k = \sqrt{k_x^2 + k_y^2 + k_z^2} = |\lambda|$. The nodal surface is protected by the γ^5 symmetry against perturbations since two bands that cross each other have different γ^5 eigenvalues and cannot be hybridized. Under a generic γ^5 -symmetric perturbation the sphere will deform and move away from $E = 0$, but will not be gapped out. On the other hand, by adding a mass term $\sim \gamma^0 = \sigma^x \otimes \tau^0$ to the Hamiltonian (1) the symmetry is broken and the nodal sphere disappears. This behavior can be understood from topology, as we will explain in the following.

On a zero-dimensional ($d_m = 0$) enclosing manifold (Fig. 1 a) an integer-valued topological invariant tied to the γ^5 symmetry can be defined as the γ^5 quantum number of the lower band that generates the nodal sphere (in our model this is the highest occupied band below $E = 0$). Given a normalized Bloch state $|u(\mathbf{k})\rangle$ of this band, we define

$$c_0(\mathbf{k}) = \langle u(\mathbf{k}) | \gamma^5 | u(\mathbf{k}) \rangle. \quad (3)$$

If this band is degenerate in energy, the γ^5 quantum numbers of individual bands should be summed and thus the topological number is \mathbb{Z} -valued. In the presence of a nodal surface one can define the difference $\Delta c_0 = c_0(\mathbf{k}_{\text{in}}) - c_0(\mathbf{k}_{\text{out}})$, where the momentum $\mathbf{k}_{\text{in}}(\text{out})$ is located inside (outside) the nodal surface, respectively. Since the highest filled band has opposite γ^5 quantum numbers outside and inside the nodal surface, the difference Δc_0 is nontrivial. As discussed in Sec. I, this difference protects the nodal surface from being gapped out by any small γ^5 -preserving perturbation.

In addition, an integer-valued topological invariant can be defined on a two-dimensional ($d_m = 2$) manifold enclosing the nodal sphere (Fig. 1 c). This is the Chern number of the lower band that generates the nodal sphere (highest occupied band below $E < 0$)

$$c_2 = \frac{i}{2\pi} \int_{S^2} d^2k d\mathcal{A}, \quad (4)$$

where the Berry connection $\mathcal{A} = \langle u(\mathbf{k}) | du(\mathbf{k}) \rangle$. In the model (1) this Chern number is nontrivial but does not change as the radius of the enclosing manifolds crosses the nodal sphere, i.e., $c_2^{\text{in}} = c_2^{\text{out}}$. Since the difference of the Chern numbers (4) inside and outside the nodal sphere is zero, we conclude that the nodal surface in this model has no robustness with respect to a generic perturbation that breaks γ^5 symmetry. Such perturbation, as for example the mass term $\sim \gamma^0 = \sigma^x \otimes \tau^0$, fully gaps out the nodal surface.

We now investigate the surface states in the model (1). Imagine that the system has a boundary at $z = 0$ and fills only a half-space $z > 0$. Due to γ^5 symmetry the Hamiltonian (1) splits into two independent Weyl blocks and thus one expects two degenerate Fermi arcs starting at the nodal surface that are protected by γ^5 symmetry. This can be demonstrated analytically by first introducing the following boundary condition $\sigma^0 \otimes \tau^x \psi = \psi$ that preserves helicity of excitations, but breaks rotational symmetry on the boundary surface. In the spirit of²⁸, we extend the boundary condition also into the bulk. Solving the Schrödinger equation $\mathcal{H}\psi_{\mp} = E\psi_{\mp}$, where \mathcal{H} is given by Eq. (1) gives the surface states $\psi_- = (\phi_-, 0)^T$ and $\psi_+ = (0, \phi_+)^T$ with

$$\phi_{\mp} = \exp(\pm i[E \mp \lambda]x + iky - kz)\phi^0, \quad (5)$$

where ϕ^0 is a constant spinor that satisfies $\tau^x \phi^0 = \phi^0$. For $k > 0$ these solutions are localized close to the boundary. If we set $E = 0$, we find two degenerate Fermi arcs

living at $(k_x, k_y) = (-\lambda, k)$. They both start ($k = 0$) on the boundary Fermi circle obtained by projecting the nodal sphere to the boundary BZ. The surface states become more and more localized as k increases. The two Fermi arcs ψ_{\mp} have opposite γ^5 eigenvalues and counter-propagate along the x axis. These counter-propagating surface modes are robust under γ^5 -symmetric perturbations \mathcal{H}_{imp} since $\langle \psi_- | \mathcal{H}_{\text{imp}} | \psi_+ \rangle = 0$.

Since the doubled Hamiltonian $\mathcal{H} \otimes \mathbb{1}_{2 \times 2}$ supports two pairs of counter-propagating modes which are robust under γ^5 symmetry-preserving perturbations, we will now look for a \mathbb{Z} -valued topological invariant protecting these surface states. In our representation the Hamiltonian (1) is block-diagonal. Every two-by-two block carries a γ^5 quantum number and can be characterized by its own topological invariant. Since the two blocks represent two Weyl points of opposite chirality doped to opposite chemical potential $\pm\lambda$, the appropriate topological invariants for the blocks are \mathbb{Z} -valued Chern numbers. These are defined only in the presence of the γ^5 symmetry and can be computed from the version of Eq. (17) (see below), where only the bands of a given block are taken into account. We emphasize that the block Chern numbers are different from the Chern number of the upper filled band (4) defined above. The absolute value of the block Chern numbers is unity (zero) for enclosing manifolds of radius larger (smaller) than the radius of the nodal sphere. These topological invariants fix the number of pairs of counter-propagating surface states in this model.

The continuum model (1) cannot be extended to the full BZ since it violates its periodicity. We conclude this section with a discussion of a minimal lattice realization of this model. The first-quantized lattice Hamiltonian that we consider has the form

$$\begin{aligned} \mathcal{H}(\mathbf{k}) = & - \left([2 - \cos k_y - \cos k_z] + 2t[\cos k_x - \cos k_0] \right) \alpha^x \\ & - 2t \sin k_y \alpha^y - 2t \sin k_z \alpha^z - \lambda \gamma^5. \end{aligned} \quad (6)$$

The model originates from the minimal lattice model of Weyl semimetals introduced in¹³ and discussed extensively in²⁹. As sketched in Fig. 2, the lattice model has two pairs of Weyl points located at $\mathbf{k} = (\pm k_0, 0, 0)$. Due to the $U(1)$ symmetry only Weyl points of the same γ^5 quantum number can be connected to each other. Hence the Nielsen-Ninomiya theorem must be applied in the two γ^5 sectors separately and nodal spheres appear necessarily in pairs.

Since there are two nodal surfaces in the minimal lattice realization, it is natural to expect that the Fermi arcs that we found above will connect the two nodal surfaces projected on the boundary BZ (see Fig. 3 a). This is indeed what one finds by diagonalizing numerically the lattice Hamiltonian in a slab geometry (see Fig. 3 b). The Fermi arcs are indeed protected by the γ^5 symmetry since by adding a mass term $\sim \sigma^x \otimes \tau^0$ to the lattice Hamiltonian (6), the Fermi arcs hybridize and gap out.

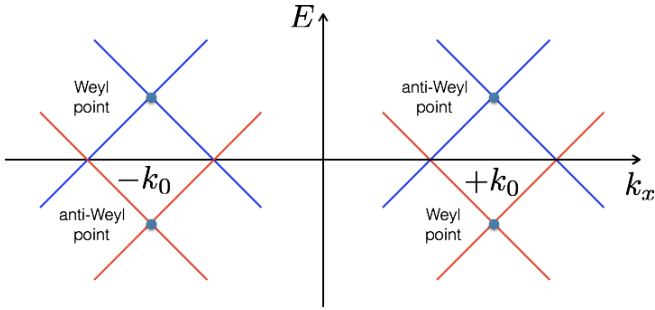


FIG. 2. Schematic spectrum of the lattice model (6) for $t, \lambda > 0$: Red and blue bands have γ^5 quantum number $+1$ and -1 and cannot be hybridized and connect to each other.

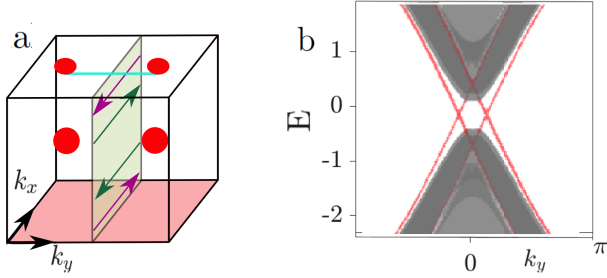


FIG. 3. Fermi arcs in a slab geometry: (a) A degenerate pair of counter-propagating surface Fermi arcs (cyan) on the upper boundary connecting the projections of nodal Fermi surfaces (for simplicity the Fermi arcs on the lower boundary are not displayed); (b) Fermi arcs (red) in the energy spectrum of the Hamiltonian (6). The counter-propagating surface states has opposite γ^5 quantum numbers and cannot be hybridized by symmetry-preserving perturbations.

B. Nodal torus

It is straightforward to modify the Hamiltonian (1) and deform the nodal sphere into a nodal torus. To this end we start from a four-band model with the effective low-energy Hamiltonian

$$\mathcal{H}(\mathbf{k}) = (k_\perp - k_0)\alpha^x + k_z\alpha^y - \lambda\gamma^5 \quad (7)$$

with $k_\perp = \sqrt{k_x^2 + k_y^2}$. The model is invariant under γ^5 symmetry. The last term in Eq. (7) splits the Dirac loop of radius k_0 at $k_z = 0$ into a pair of Weyl loops by separating them in energy by an amount of 2λ . The dispersion relation for this system is

$$E = \pm\sqrt{(k_\perp - k_0)^2 + k_z^2} \pm \lambda \quad (8)$$

and exhibits a band degeneracy at $E = 0$ with $\sqrt{(k_\perp - k_0)^2 + k_z^2} = \lambda$ which for $\lambda < k_0$ forms a torus in momentum space.

In a close analogy to the nodal sphere discussed in Sec. II A, the nodal torus is protected by the unitary γ^5

symmetry. The appropriate \mathbb{Z} -valued topological invariant defined on a zero-dimensional enclosing manifold is given by Eq. (4). For the model (7) the difference of the invariants defined inside and outside the nodal torus is nontrivial which ensures its full robustness under small γ^5 -preserving perturbations. The Chern number (4) is zero at any enclosing manifold and hence a nodal torus has no robustness under arbitrary small perturbations.

Contrary to the nodal sphere model the nodal torus does not support zero-energy surface states. Notice that the two-by-two diagonal blocks of the Hamiltonian (7) are not invariant under chiral sub-lattice symmetry for $\lambda \neq 0$. As a result the topological AIII winding number^{3,30} cannot be defined for these blocks in the presence of a finite γ^5 term in the Hamiltonian. As a physical consequence, the pair of flat-band drumhead zero-energy surface states present in a chiral-symmetric Dirac loop system ($\lambda = 0$) are shifted away from zero energy by the γ^5 term in the Hamiltonian (7). Incidentally, the blocks of the Hamiltonian (7) give rise to the π Berry phase on a one-dimensional exterior manifold that links with the nodal torus. As explained in³¹ the quantization of the Berry phase is not robust and is a consequence of an accidental symmetry.

In order to strengthen the arguments above, we consider a minimal lattice model that realizes a nodal torus. Its Hamiltonian reads

$$\begin{aligned} \mathcal{H}(\mathbf{k}) = & - \left(6t - k_0^2 - 2t \cos k_x - 2t \cos k_y - 2t \cos k_z \right) \alpha^x \\ & - 2t \sin k_z \alpha^y - \lambda \gamma^5. \end{aligned} \quad (9)$$

and is motivated by the lattice model of a nodal loop semimetal investigated in³². The bulk energy spectrum of this Hamiltonian is shown in Fig. 4 a. It is worth pointing out that this lattice model has just one nodal torus in the BZ. Hence there is no Nielsen-Ninomiya doubling for nodal tori and the block Chern numbers are trivial in this case. We also evaluated the energy spectrum of the lattice Hamiltonian in a slab geometry, see Fig. 4 band found no zero-energy surface states.

III. NODAL SURFACES PROTECTED BY ANTI-UNITARY SYMMETRY

Here we turn to four-band models that exhibit nodal surfaces which are protected by anti-unitary symmetries. These objects appeared in the recent literature¹⁷⁻¹⁹ and formed the starting point of our investigation.

A. Nodal sphere

Consider a four-band model with the Hamiltonian

$$\mathcal{H}(\mathbf{k}) = k_i \tilde{\alpha}^i - \lambda \gamma^5 - \delta \gamma^0, \quad (10)$$

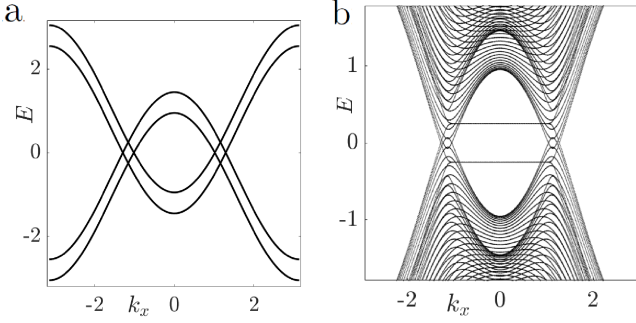


FIG. 4. Energy spectrum of the lattice model (9): (a) Infinite system: the nodal torus is projected on the energy-momentum plane as four intersections of the bands at $E = 0$; (b) Slab geometry: the flat band surface states are separated in energy by the γ^5 term in the Hamiltonian.

where $\tilde{\alpha}^i = \sigma^0 \otimes \tau^i$, $\gamma^5 = -\sigma^z \otimes \tau^0$ and $\gamma^0 = \sigma^x \otimes \tau^0$. The model consists of a pair of Weyl points of the same chirality which are split in energy by the last two terms in Eq. (10). Notice that the Hamiltonian has no unitary $U(1)$ symmetry apart from the particle number conservation. Even in the absence of a unitary symmetry, the spectrum of the Hamiltonian (10)

$$E = \pm k \pm \sqrt{\lambda^2 + \delta^2} \quad (11)$$

contains a band degeneracy at $E = 0$ which is located on a sphere of radius $k = \sqrt{\lambda^2 + \delta^2}$.

We will argue now that in this model the nodal surface is protected by an anti-unitary combination of inversion P and particle-hole C symmetry^{33,34} and construct a \mathbb{Z}_2 -valued topological invariant tied to this symmetry^{17,19}. To this end consider a class of Hamiltonians of the form

$$\mathcal{H}(\mathbf{k}) = a_i(\mathbf{k})\tilde{\alpha}^i + b_i(\mathbf{k})\tilde{\beta}^i \quad (12)$$

with $\tilde{\alpha}^i = \sigma^0 \otimes \tau^i$ and $\tilde{\beta}^i = \sigma^i \otimes \tau^0$ and \mathbf{a} and \mathbf{b} being real functions of \mathbf{k} . The model (10) is a special case of (12) since $\gamma^0 = \tilde{\beta}^x$ and $\gamma^5 = -\tilde{\beta}^z$. It will turn out important in the following that the Hamiltonian (12) can be unitary rotated to an antisymmetric form^{17,19} to be denoted by $\bar{\mathcal{H}}$. The spectrum of (12)

$$E = \pm |\mathbf{a}(\mathbf{k})| \pm |\mathbf{b}(\mathbf{k})| \quad (13)$$

supports a zero-energy nodal surface at $|\mathbf{a}(\mathbf{k})| = |\mathbf{b}(\mathbf{k})|$. A generic model (12) breaks inversion P , time-reversal T and particle-hole C symmetries. Nevertheless, it is invariant under the anti-unitary PC symmetry which acts on the Hamiltonian as

$$U_{PC}\mathcal{H}^*(\mathbf{k})U_{PC}^{-1} = -\mathcal{H}(\mathbf{k}). \quad (14)$$

In our representation $U_{PC} = \sigma^y \otimes \tau^y$ is a real. Note that $(PC)^2 = U_{PC}U_{PC}^* = +\mathbb{1}$. Due to this symmetry the

nodal surface is fixed to the Fermi level and thus necessarily coincides with the Fermi surfaces of the two touching bands. It was found in^{33,34} that three-dimensional Fermi surfaces with PC symmetry that squares to unity have topological \mathbb{Z}_2 classification. In our formulation, the topological invariant defined on a zero-dimensional enclosing manifold can be calculated as the sign of the Pfaffian of the antisymmetric form of the Hamiltonian $\bar{\mathcal{H}}$

$$c_0(\mathbf{k}) = \text{sgn} \text{Pf} \bar{\mathcal{H}}(\mathbf{k}). \quad (15)$$

Since in our representation the Hamiltonian (12) is not antisymmetric, in order to compute the invariant, we must first unitary rotate it to the antisymmetric form $\bar{\mathcal{H}} = \Omega \mathcal{H} \Omega^\dagger$. The resulting Pfaffian

$$\text{Pf} \bar{\mathcal{H}} = \mathbf{b}^2(\mathbf{k}) - \mathbf{a}^2(\mathbf{k}) \quad (16)$$

is real and vanishes on the nodal surface. In particular, for the model (10) the Pfaffian has a simple zero on the nodal sphere and thus it has opposite signs inside and outside of it. Following the arguments of Sec. I, the nontrivial difference of the Pfaffians makes the nodal sphere fully robust with respect to small PC -invariant perturbations. We notice that although the choice of Ω and the sign of the resulting $c_0(\mathbf{k})$ is not unique, this ambiguity does not affect the difference of the topological invariants.

We discuss now the Chern number invariant (4) in the context of the model (10). For an enclosing manifold located inside (outside) the nodal sphere the band Chern number is nontrivial and in addition $c_2^{\text{in}} = -c_2^{\text{out}}$. The nontrivial difference of the band Chern numbers $\Delta c_2 = c_2^{\text{in}} - c_2^{\text{out}}$ ensures that a generic small perturbation cannot fully gap out the nodal sphere, but has to leave in the band structure at least a pair of Weyl points close to the Fermi level. Thus contrary to the nodal objects from Sec. II, the nodal sphere discussed here has certain robustness with respect to arbitrary perturbations of the Hamiltonian.

In the presence of a spatial boundary, for $\lambda = \delta = 0$ in Eq. (10) a pair of same-chirality Weyl points at the Fermi level gives rise to a pair of chiral co-propagating zero-energy Fermi arcs. As the Weyl points are split in energy for $\lambda, \delta \neq 0$, the Fermi arcs survive but must start at the Fermi surfaces. These surface states are robust against arbitrary small perturbations thanks to the the total Chern number

$$\text{total Chern number} = \frac{i}{2\pi} \int_{S^2} d^2k \text{tr} \mathcal{F} \quad (17)$$

which is nontrivial on an enclosing manifold outside the Fermi surfaces. Here the Berry curvature two-form $\mathcal{F} = d\mathcal{A} + \mathcal{A} \wedge \mathcal{A}$ is defined in terms of the non-abelian Berry connection $\mathcal{A}^{ab} = \langle u^a(\mathbf{k}) | du^b(\mathbf{k}) \rangle$, where a, b label only occupied bands. On an enclosing manifold living inside the nodal sphere the total Chern number (17) vanishes and thus the nodal sphere represents a locus of the total Berry flux. It is an inflated double Weyl monopole¹⁷.

Due to the Nielsen-Ninomiya theorem the nodal spheres protected by the anti-unitary PC symmetry should always appear in pairs. To demonstrate it explicitly we considered the minimal lattice Hamiltonian

$$\begin{aligned}\mathcal{H}(\mathbf{k}) = & - \left([2 - \cos k_y - \cos k_z] + 2t[\cos k_x - \cos k_0] \right) \tilde{\alpha}^x \\ & - 2t \sin k_y \tilde{\alpha}^y - 2t \sin k_z \tilde{\alpha}^z - \delta \gamma^0 - \lambda \gamma^5.\end{aligned}\quad (18)$$

and determined numerically its energy spectrum in the bulk. In addition, we examined the energy spectrum of this lattice Hamiltonian in a slab geometry. As expected, it contains a pair of chiral zero-energy Fermi arcs which are robust with respect to arbitrary perturbations of the Hamiltonian.

B. Nodal torus

Finally we construct and analyze a four-band model that exhibits a nodal torus that is protected by anti-unitary symmetry. The model is defined by the real Hamiltonian

$$\mathcal{H}(\mathbf{k}) = (k_{\perp} - k_0) \tilde{\alpha}^x + k_z \tilde{\alpha}^z - \lambda \gamma^5 - \delta \gamma^0 \quad (19)$$

with $k_{\perp} = \sqrt{k_x^2 + k_y^2}$. Apart from the particle number symmetry, there is no $U(1)$ symmetry. Nevertheless the energy spectrum

$$E = \pm \sqrt{(k_{\perp} - k_0)^2 + k_z^2} \pm \sqrt{\lambda^2 + \delta^2} \quad (20)$$

has a zero-energy band degeneracy at $\sqrt{(k_{\perp} - k_0)^2 + k_z^2} = \sqrt{\lambda^2 + \delta^2}$ forming a torus in momentum space for $\sqrt{\lambda^2 + \delta^2} < k_0$.

Since the model (19) falls into the class of PC -symmetric Hamiltonians (12), similar to the nodal sphere discussed in section III A, one can define the Pfaffian \mathbb{Z}_2 invariant (15). By evaluating the Pfaffian (16) in the model (19), one finds that the difference of the Pfaffian invariant inside and outside the nodal torus is non-trivial and thus this object cannot be gapped out by small PC -invariant perturbations of the Hamiltonian.

Incidentally, the model (19) enjoys more symmetries. The Hamiltonian is real that implies the anti-unitary PT symmetry that acts on the Hamiltonian as

$$\mathcal{H}^*(\mathbf{k}) = \mathcal{H}(\mathbf{k}) \quad (21)$$

and squares to unity. This symmetry together with the anti-unitary PC symmetry implies the unitary chiral sublattice (anti)symmetry of the model (19)

$$\{\mathcal{H}(\mathbf{k}), U_S\} = 0, \quad U_S = \sigma^y \otimes \tau^y \quad (22)$$

and gives rise to a winding number topological invariant introduced in¹⁹. In order to construct this invariant, it is convenient to perform a unitary rotation Ω

which diagonalizes the chiral sublattice symmetry operator $S \rightarrow \Omega^\dagger S \Omega = \sigma^z \otimes \tau^0$. This transformation brings the Hamiltonian into the block off-diagonal form

$$\mathcal{H}(\mathbf{k}) = \begin{pmatrix} 0 & h(\mathbf{k}) \\ h^\dagger(\mathbf{k}) & 0 \end{pmatrix}, \quad (23)$$

Here due to the PT symmetry the block Hamiltonian h is real. To proceed, it is useful to define a flattened Hamiltonian which for a general non-interacting fermionic system with n filled and m empty bands reads

$$Q(\mathbf{k}) = U(\mathbf{k}) \begin{pmatrix} \mathbb{1}_{m \times m} & 0 \\ 0 & -\mathbb{1}_{n \times n} \end{pmatrix} U^\dagger(\mathbf{k}), \quad (24)$$

where the unitary matrix $U(\mathbf{k})$ diagonalizes the Hamiltonian

$$\begin{aligned}U^\dagger(\mathbf{k}) \mathcal{H}(\mathbf{k}) U(\mathbf{k}) = \\ = \underbrace{\text{diag}(\epsilon_{m+n}(\mathbf{k}), \dots, \epsilon_{n+1}(\mathbf{k}), \epsilon_n(\mathbf{k}), \dots, \epsilon_1(\mathbf{k}))}_{\text{empty bands}} \underbrace{\epsilon_m(\mathbf{k}), \dots, \epsilon_1(\mathbf{k})}_{\text{filled bands}}.\end{aligned}\quad (25)$$

The flattened Hamiltonian $Q(\mathbf{k})$ is well-defined only away from band degeneracies. In the presence of the chiral sublattice symmetry $m = n$ and the flattened Hamiltonian is block off-diagonal

$$Q(\mathbf{k}) = \begin{pmatrix} 0 & q(\mathbf{k}) \\ q^\dagger(\mathbf{k}) & 0 \end{pmatrix} \quad (26)$$

in any basis which diagonalizes the operator S . Note that in general $q(\mathbf{k}) \in \text{U}(n)$ since $Q^2 = \mathbb{1}$. The additional reality condition (21) that follows from the PT symmetry implies that the flattened block $q(\mathbf{k}) \in \text{O}(n)$. In particular, for the four-band model (19) one has $q(\mathbf{k}) \in \text{O}(2)$. Now on any closed one-dimensional manifold that does not intersect the torus in the BZ one can compute the topological winding number¹⁹ as the homotopy equivalence class of mappings $S^1 \rightarrow SO(2)$. We define the winding number as

$$c_1 = -\frac{i}{4\pi} \oint ds \text{Tr} [q^T \sigma^y \partial_s q], \quad (27)$$

where s is a coordinate that parametrizes the one-dimensional enclosing manifold. The invariant is integer-valued since the homotopy group $\pi_1[SO(2)] = \mathbb{Z}^{35}$. It is instructive now to evaluate the winding number invariant for the nodal torus model (19). To this end we consider an enclosing S^1 manifold of radius k_S that is positioned in the $x - z$ plane and is centered at the momentum $\mathbf{k} = (k_0, 0, 0)$. A straightforward calculation reveals that if $k_S > \sqrt{\lambda^2 + \delta^2}$, i.e., the manifold encloses the torus from outside and links with it, the absolute value of the winding number c_1^{out} is equal to unity. On the other hand for $k_S < \sqrt{\lambda^2 + \delta^2}$, the winding number c_1^{in} vanishes since in this case the enclosing manifold can be shrunk to a point without crossing energy bands. Following general

arguments from Sec. I, the nontrivial difference of the winding numbers ensures that the nodal torus cannot be fully gapped out by small perturbations that are invariant under PC and PT symmetries. Note however that in the present case this prediction has little practical value because the nodal torus is fully protected against any small PC -symmetric perturbation by the Pfaffian invariant. It would be interesting to find a model protected by the nontrivial difference of topological invariant defined on one-dimensional enclosing manifolds, where a nodal surface is gapped out to nodal loop(s).

Finally, we observe that similar to the model discussed in Sec. II B, the present model does not support robust zero-energy surface states. The pair of zero-energy drum-head surface states present in the limit of the double-Weyl loop ($\lambda = \delta = 0$) is shifted to a finite energy by the last two terms in the Hamiltonian (19). One arrives to the same conclusion by diagonalizing the lattice the Hamiltonian

$$\mathcal{H} = - \left(6t - k_0^2 - 2t \cos k_x - 2t \cos k_y - 2t \cos k_z \right) \tilde{\alpha}^x - 2t \sin k_z \tilde{\alpha}^z - \lambda \gamma^5 - \delta \gamma^0 \quad (28)$$

in a slab geometry.

IV. CONCLUSION AND OUTLOOK

In this paper we investigated the physics of three-dimensional fermionic band models that exhibit two-dimensional Weyl nodal surfaces. We argued that the robustness of these nodal objects is ensured by topology. Specifically, we showed that the degree of robustness is determined by the dimensionality of gapped enclosing manifolds, where topological invariants are evaluated. We demonstrated this in several four-band toy models that exhibit nodal surfaces protected by unitary or anti-unitary symmetry. It would be interesting to find realistic models of materials where these ideas can be applied.

ACKNOWLEDGMENTS:

We acknowledge fruitful discussions with Barry Bradlyn, Anton Burkov, Tomáš Bzdušek and Titus Neupert. Our work is supported by the Emmy Noether Programme of German Research Foundation (DFG) under grant No. MO 3013/1-1.

Appendix A: Topological robustness of general nodal surfaces

Although in the main part of the paper we limit our attention to nodal surfaces tuned to the Fermi level,

this assumption is not necessary and general (dispersing in energy) nodal surfaces exhibit topological robustness to small perturbations in the way we put forward in Sec. I. To understand the dispersing case, it is useful to consider a four-dimensional energy-momentum space which is naturally partitioned by three-dimensional energy bands into four-dimensional regions. If a topological invariant of the band structure can be defined on a manifold residing in some four-dimensional region, by construction it must be constant within the given region. In general, a nontrivial difference of topological invariants evaluated on enclosing manifolds of dimensions $d_m = 0, 1, 2$ embedded in different properly chosen regions of the energy-momentum space guarantees a nodal object of dimension $d = 2, 1, 0$ in the presence of any small perturbation compatible with the given topological invariant. For the case $d_m = 0$, the mechanism is illustrated in Fig. 5.

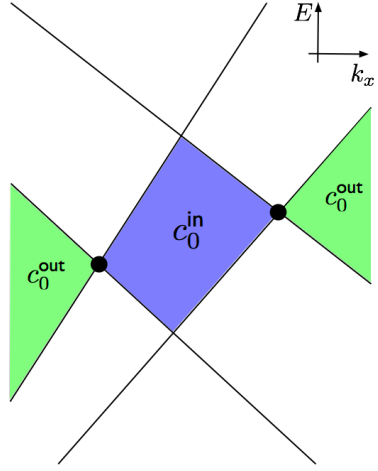


FIG. 5. A two-dimensional cut of the four-dimensional energy-momentum space partitioned by bands (black solid lines) into regions. The nodal surface projects as two black dots on the cut. Nontrivial difference of topological invariants c_0^{out} and c_0^{in} defined on any two zero-dimensional point manifolds located within the outer (green) and inner (blue) regions, respectively, protects the nodal surface from being gapped.

¹ M. Z. Hasan and C. L. Kane, Rev. Mod. Phys. **82**, 3045 (2010).

² X.-L. Qi and S.-C. Zhang, Rev. Mod. Phys. **83**, 1057 (2011).

³ A. P. Schnyder, S. Ryu, A. Furusaki, and A. W. W. Ludwig, Phys. Rev. B **78**, 195125 (2008).

⁴ A. M. Turner and A. Vishwanath, arXiv:1301.0330.

⁵ A. Burkov, Journal of Physics: Condensed Matter **27**, 113201 (2015).

⁶ N. P. Armitage, E. J. Mele, and A. Vishwanath, arXiv:1705.01111.

⁷ G. E. Volovik, *Exotic properties of superfluid ^3He* , Vol. 1 (World Scientific, 1992).

⁸ G. E. Volovik, *The universe in a helium droplet*, Vol. 117 (Oxford University Press New York, 2009).

⁹ S.-Y. Xu, I. Belopolski, N. Alidoust, M. Neupane, G. Bian, C. Zhang, R. Sankar, G. Chang, Z. Yuan, C.-C. Lee, *et al.*, Science **349**, 613 (2015).

¹⁰ B. Q. Lv, H. M. Weng, B. B. Fu, X. P. Wang, H. Miao, J. Ma, P. Richard, X. C. Huang, L. X. Zhao, G. F. Chen, Z. Fang, X. Dai, T. Qian, and H. Ding, Phys. Rev. X **5**, 031013 (2015).

¹¹ H. B. Nielsen and M. Ninomiya, Physics Letters B **105**, 219 (1981).

¹² D. T. Son and B. Z. Spivak, Phys. Rev. B **88**, 104412 (2013).

¹³ K.-Y. Yang, Y.-M. Lu, and Y. Ran, Phys. Rev. B **84**, 075129 (2011).

¹⁴ X. Wan, A. M. Turner, A. Vishwanath, and S. Y. Savrasov, Phys. Rev. B **83**, 205101 (2011).

¹⁵ A. A. Burkov, M. D. Hook, and L. Balents, Phys. Rev. B **84**, 235126 (2011).

¹⁶ Y. Kim, B. J. Wieder, C. L. Kane, and A. M. Rappe, Phys. Rev. Lett. **115**, 036806 (2015).

¹⁷ D. F. Agterberg, P. M. R. Brydon, and C. Timm, Phys. Rev. Lett. **118**, 127001 (2017).

¹⁸ C. Timm, A. P. Schnyder, D. F. Agterberg, and P. M. R. Brydon, arXiv:1707.02739.

¹⁹ T. Bzdušek and M. Sigrist, arXiv:1705.07126.

²⁰ One can imagine a scenario where a closed nodal surface is partially gapped to a nodal surface with boundaries. This case is not discussed in this paper.

²¹ C. Fang, Y. Chen, H.-Y. Kee, and L. Fu, Phys. Rev. B **92**, 081201 (2015).

²² C. Fang, H. Weng, X. Dai, and Z. Fang, Chin Phys B **25**, 117106 (2016).

²³ P. Hořava, Phys. Rev. Lett. **95**, 016405 (2005).

²⁴ Y. X. Zhao and Z. D. Wang, Phys. Rev. Lett. **110**, 240404 (2013).

²⁵ S. Matsuura, P.-Y. Chang, A. P. Schnyder, and S. Ryu, New J. Phys. **15**, 065001 (2013).

²⁶ In high energy physics this is known as the axial symmetry.

²⁷ K. Fukushima, D. E. Kharzeev, and H. J. Warringa, Phys. Rev. D **78**, 74033 (2008).

²⁸ E. Witten, Nuovo Cimento Rivista Serie **39**, 313 (2016), arXiv:1510.07698.

²⁹ T. M. McCormick, I. Kimchi, and N. Trivedi, Phys. Rev. B **95**, 075133 (2017).

³⁰ S. Ryu, A. P. Schnyder, A. Furusaki, and A. W. W. Ludwig, New J. Phys. **12**, 065010 (2010).

³¹ O. Türker, *Nodal surface metals*, Master's thesis, TUM (2017).

³² Y. Wang and R. M. Nandkishore, Phys. Rev. B **95**, 060506 (2017).

³³ S. Kobayashi, K. Shiozaki, Y. Tanaka, and M. Sato, Phys. Rev. B **90**, 024516 (2014).

³⁴ Y. X. Zhao, A. P. Schnyder, and Z. D. Wang, Phys. Rev. Lett. **116**, 156402 (2016).

³⁵ Since $\pi_1[SO(n)] = \mathbb{Z}_2$ for $n > 2$, the winding number is only \mathbb{Z}_2 -valued for models with more than four bands¹⁹.